

# The Ewing Amputation: The First Human Implementation of the Agonist-Antagonist Myoneural Interface

Tyler R. Clites, PhD\*  
 Hugh M. Herr, PhD\*  
 Shriya S. Srinivasan, BS\*  
 Anthony N. Zorzos, PhD\*  
 Matthew J. Carty, MD\*†

**Background:** The agonist-antagonist myoneural interface (AMI) comprises a surgical construct and neural control architecture designed to serve as a bidirectional interface, capable of reflecting proprioceptive sensation of prosthetic joint position, speed, and torque from an advanced limb prosthesis onto the central nervous system. The AMI surgical procedure has previously been vetted in animal models; we here present the surgical results of its translation to human subjects.

**Methods:** Modified unilateral below knee amputations were performed in the elective setting in 3 human subjects between July 2016 and April 2017. AMIs were constructed in each subject to control and interpret proprioception from the bionic ankle and subtalar joints. Intraoperative, perioperative, and postoperative residual-limb outcome measures were recorded and analyzed, including electromyographic and radiographic imaging of AMI musculature.

**Results:** Mean subject age was  $38 \pm 13$  years, and mean body mass index was  $29.5 \pm 5.5$  kg/m<sup>2</sup>. Mean operative time was  $346 \pm 87$  minutes, including 120 minutes of tourniquet time per subject. Complications were minor and included transient cellulitis and one instance of delayed wound healing. All subjects demonstrated mild limb hypertrophy postoperatively, and intact construct excursion with volitional muscle activation. All patients reported a high degree of phantom limb position perception with no reports of phantom pain.

**Conclusions:** The AMI offers the possibility of improved prosthetic control and restoration of muscle-tendon proprioception. Initial results in this first cohort of human patients are promising and provide evidence as to the potential role of AMIs in the care of patients requiring below knee amputation. (*Plast Reconstr Surg Glob Open* 2018;6:e1997; doi: 10.1097/GOX.0000000000001997; Published online 16 November 2018.)

## INTRODUCTION

Amputation surgery has not evolved at a pace commensurate with advances in external limb prosthetic technology, resulting in a discordance between standard

*From the \*Massachusetts Institute of Technology, Center for Extreme Bionics, Cambridge, Mass.; and †Division of Plastic Surgery, Department of Surgery, Brigham and Women's Hospital, Boston, Mass. Received for publication June 28, 2018; accepted September 14, 2018.*

*Presented at the International Symposium on Amputation Surgery and Prosthetic Technology (IASPT) 2018 in Vienna, Austria.*

*Clinical Trial registered as "Somatotopic Configuration of Distal Residual Limb Tissues in Lower Extremity Amputations", NCT03374319.*

*This study was carried out in full compliance with protocols approved by Partners IRB (protocol p2014001379) and MIT COUHES (protocol 1609692618).*

*Copyright © 2018 The Authors. Published by Wolters Kluwer Health, Inc. on behalf of The American Society of Plastic Surgeons. This is an open-access article distributed under the terms of the Creative Commons Attribution-Non Commercial-No Derivatives License 4.0 (CCBY-NC-ND), where it is permissible to download and share the work provided it is properly cited. The work cannot be changed in any way or used commercially without permission from the journal.*

DOI: 10.1097/GOX.0000000000001997

clinical practice and options for subsequent prosthetic limb replacement.<sup>1</sup> In the traditional limb amputation procedure, tissues distal to the amputation site are discarded, despite their capacity to contribute to reconstruction of the residuum. The standard practice of traction neurectomy is only partially effective in preventing neuropathic pain and creates a hurdle for neural interfaces due to inaccessibility of transected distal nerve endings.<sup>2</sup> Muscles in the residual limb are typically myodesed isometrically, severing the dynamic relationships that exist between agonist-antagonist pairs<sup>3</sup>; this fixation limits the

**Disclosure:** Dr. Herr has a consulting relationship with Ottobock. Drs. Herr and Carty are inventors on an issued patent describing the AMI concept. Drs. Herr, Carty, Clites, and Zorzos are inventors on a pending patent describing the Ewing procedure. MIT holds both patents. None of the other authors has a financial interest in any of the products, devices, or drugs mentioned in this article. The Article Processing Charge was paid for by the authors.

Supplemental digital content is available for this article. Clickable URL citations appear in the text.

ability of biological mechanoreceptors within each muscle to communicate proprioceptive information to the central nervous system. The collective result is a soft-tissue architecture that is ill suited for bi-directional neural communication between a patient's residuum and an external prosthesis, and mechanical interfacing with a socket.

Revision strategies have emerged to overcome the limitations of this traditional amputation procedure. Targeted muscle reinnervation expands the controllability of myoelectric prostheses and limits pathological neurology<sup>2,4,5</sup> but requires cannibalization of healthy muscle to provide reinnervation targets. Regenerative peripheral nerve interfaces (RPNI) provide an alternative strategy in which free muscle grafts are coapted to the distal ends of transected nerves.<sup>6-8</sup> However, neither targeted muscle reinnervation nor RPNI restore dynamic agonist-antagonist muscle relationships, limiting neural control and the ability of patients to receive proprioceptive feedback from a prosthetic limb.

The agonist-antagonist myoneural interface (AMI) is a bi-directional neural communication platform described primarily as a means of controlling and interpreting proprioceptive feedback from, a prosthetic joint.<sup>9-15</sup> An AMI comprises an agonist and antagonist muscle coapted in series, such that contraction of the agonist causes stretch in the antagonist (Fig. 1). Natural proprioceptive responses from mechanoreceptors within both muscles are generated with AMI activation, and these neural signals are interpreted by the central nervous system as sensations of joint position, speed, and torque associated with movement of the phantom joint.

Herein, we present the Ewing amputation, a new surgical procedure for below knee amputation that incorporates AMIs into the transtibial residuum. We describe patient selection, surgical technique, rehabilitation, and outcome measures for the first 3 patients treated with this amputation technique. We also provide evidence that the Ewing amputation has the potential to limit aberrant and

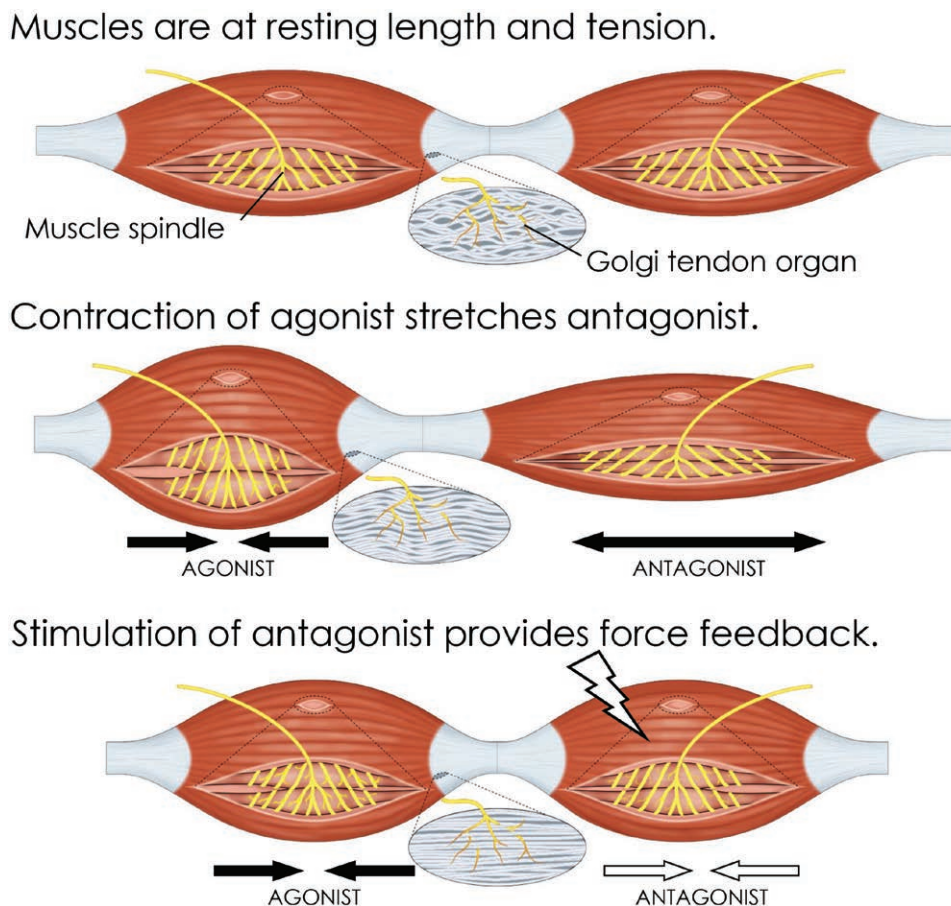


**Fig. 1.** Conceptual illustration of the AMI. Mechanical linkage of innervated muscles restores natural contracture-stretch relationships, leading to activation of native mechanoreceptors and bi-directional communication with the central nervous system. AMI function is described as follows: at rest, both AMI muscles are at resting length and tension. When the agonist muscle contracts under volitional or reflexive activation, the antagonist is passively stretched, causing increased spindle discharge in the antagonist. This spindle activity is interpreted by the central nervous system (CNS) as a change in phantom joint position. Force feedback is provided to the CNS as artificial stimulation of the antagonist muscle causes it to contract in opposition to the agonist, creating tension at the agonist musculotendinous junction and increasing agonist Golgi tendon organ (GTO) discharge. This is interpreted by the CNS as torque about the phantom joint. A representation of muscle spindle and GTO state is shown for each condition.

painful phantom symptomatology, prevent residual limb atrophy, and preserve independent volitional muscle activation.

## METHODS

### Patient Selection

Patients were recruited for enrollment under Partners IRB-approved protocol p2014001379 and MIT IRB-approved protocol 1609692618. Eligibility for inclusion was contingent upon eligibility for standard below-knee amputation due to prior traumatic injury, congenital abnormality, or malignancy; patients with peripheral vascular disease were not deemed to be eligible for inclusion due to concerns about peripheral neuropathies. Before enrollment, all patients underwent multiple clinic evaluations with the senior author, and several third party specialists. Agreement for participation in the study was then provided by each patient following review of the IRB-approved consent forms.

Three patients were selected for inclusion in this study:

- Patient 1 is a 52-year-old man with no significant past medical history who sustained multiple injuries in the context of a 50-foot fall in 2014. These injuries included a highly comminuted fracture to his left talus requiring open reduction and internal fixation, complicated by nonunion. He subsequently developed chronic pain and dysesthesias in the left foot and ankle, and intermittent ankle instability. After talus hardware removal in 2015, he experienced little improvement in pain. He was subsequently recommended for tibiotalar arthrodesis; however, due to concerns about impaired function and ongoing pain in the setting of a fusion, he opted instead for elective amputation.
- Patient 2 is a 25-year-old male Army veteran with no significant past medical history, who sustained multiple injuries in the context of an improvised explosive device (IED) detonation in 2013. These injuries included open fractures to his left tibia, fibula, and hindfoot, requiring initial external fixator placement followed by definitive open reduction and internal fixation of the tibia, and subtalar fusion with bone grafting. He subsequently required dynamization for tibial nonunion. Thereafter, he experienced chronic left ankle neuropathic pain and instability, for which he underwent tibial hardware removal with little improvement. He was subsequently recommended for elective below knee amputation.
- Patient 3 is a 36-year-old man with a congenital left clubfoot deformity, resulting in a prolonged history of recurrent metatarsal fractures throughout childhood and adolescence. At the age of 21, he underwent triple arthrodesis osteotomies and Achilles lengthening, complicated by nonunion. In 2015, he underwent a gastrocnemius recession, talonavicular fusion, navicular medial cuneiform fusion, calcaneocuboid fusion, and tibial bone graft harvesting that was complicated by extensive avascular necrosis of his talus. He thereafter experienced unrelenting pain and instability in the left ankle and was subsequently recommended for elective below knee amputation.

### Surgical Technique

All amputation procedures were performed with the patient in the supine position, under general anesthesia, sterile conditions, and tourniquet control. Preoperative intravenous antibiotics were administered in all cases. Preoperative measurements of lower limb circumference were made 6 cm and 12 cm distal to the tibial plateau. A standard stair-step incision was made approximately 12 cm distal to the tibial plateau, preserving a posterior fasciocutaneous flap extending to the distal Achilles. Dissection was carried down to the underlying muscle fascia. Each of the leg compartments was explored to identify the tibialis anterior (TA), lateral gastrocnemius, peroneus longus, and tibialis posterior muscles. These muscles were marked at resting tension with the ankle and subtalar joints in their neutral positions using sutures set at 1 cm intervals. All muscles of the anterior, lateral, and posterior (both superficial and deep) compartments were disinserted. The distal ends of the tibial, superficial peroneal, deep peroneal, and sural nerves were identified, isolated, and transected. Dissection was carried down to the level of the periosteum of the tibia and fibula, and osteotomies were made at approximately 12 cm and 10 cm, respectively. The anterior tibial, posterior tibial, and peroneal vessels were ligated. The medial and lateral tarsal tunnels were procured from the distal amputated limb via sharp dissection, including 4–5 cm segments of each tunnel's native tendon contents, and were affixed to the flat of the residual tibia using multiple unicortical suture anchors. AMIs were constructed via coaptation of the TA and lateral gastrocnemius muscles to either end of the tendon portion passing through the proximally positioned tarsal tunnel, and coaptation of the tibialis posterior and peroneus longus muscles to the distally positioned tarsal tunnel. Radiopaque 1–2 mm tantalum beads were embedded in the center of each tarsal tunnel, and in all 4 AMI muscles. In patients 2 and 3, the distal ends of the tibial, superficial peroneal, deep peroneal, and sural nerves were capped with free muscle grafts harvested from the distal amputated limb to establish neuroma-preventing RPNIs. The soft-tissue envelope was then closed in a layered fashion over a single closed suction drain. Finally, a layered compression dressing and standard knee immobilizer was applied (Figs. 2–4).

### Postoperative Recovery

All patients were admitted to the inpatient ward following their operative procedure. Postoperative intravenous antibiotics and analgesics were provided for the duration of admission. All were discharged to home following achievement of standard clinical milestones. Outpatient follow-up occurred weekly for all patients until suture removal and adequate surgical site healing, at which point all patients were cleared to begin standard prosthesis fitting.

All patients were enlisted in a modified postoperative rehabilitation program that included strengthening and range of motion exercises typical of a standard below knee amputation regimen, and targeted muscle recruitment and cognitive training exercises designed to facilitate motion and perception in the AMI constructs (see figure, **Supplemental Digital Content 1**, which displays multimodal



**Fig. 2.** Operative technique. A, Standard below knee amputation incision pattern. B, Tension marking sutures on component muscles. C, Disinsertion of component muscles. D, Isolation of tibia and fibula in preparation for osteotomies. E, Harvesting of tarsal tunnels from amputated distal limb. F, Tarsal tunnel with native tendon component. G, Placement of suture anchors for tarsal tunnel fixation to anterior tibia. H, Position of tarsal tunnels on anterior tibia following fixation.



**Fig. 3.** Displays operative site closure.

rehabilitation regimen including preoperative training and cognitive conditioning, <http://links.lww.com/PRSGO/A911>). All patients began rehabilitation under the guidance of a certified physical therapist at postoperative week 4.

**Data Collection**

Clinical data were collected during each patient’s peri-operative period and subsequent follow-up visits. Imaging of all residual limbs was performed postoperatively, and included plain radiographs, fluoroscopy, and ultrasound. Subjective questioning regarding phantom symptomatology and proprioception was performed in conjunction with all imaging studies.

Experimental evaluation of each patient’s residual limb function was performed using a combination of electromyography (EMG) and high-resolution ultrasound. These assessments were conducted as follows:

- **EMG:** Independent control of muscle activation was evaluated as each subject moved his phantom ankle and subtalar joints to approximately 80% dorsiflexion, plantar flexion, inversion, and eversion. Each position was held for 3 seconds before returning to rest. During these motions, EMG was recorded simultaneously from each of the 4 muscles via bipolar surface electrodes (Trigno, Delsys). Raw EMG was high-pass filtered at 70 Hz, full-wave rectified, and integrated using a 100 ms moving average window. Amplitude of this integrated signal was calibrated to maximum voluntary contraction; this normalized EMG signal amplitude was then averaged across the “hold” portion of each motion, providing an estimate of activation for each muscle. Auxiliary muscle activation was calculated as the net activation in the AMI not associated with the desired movement (eg, during

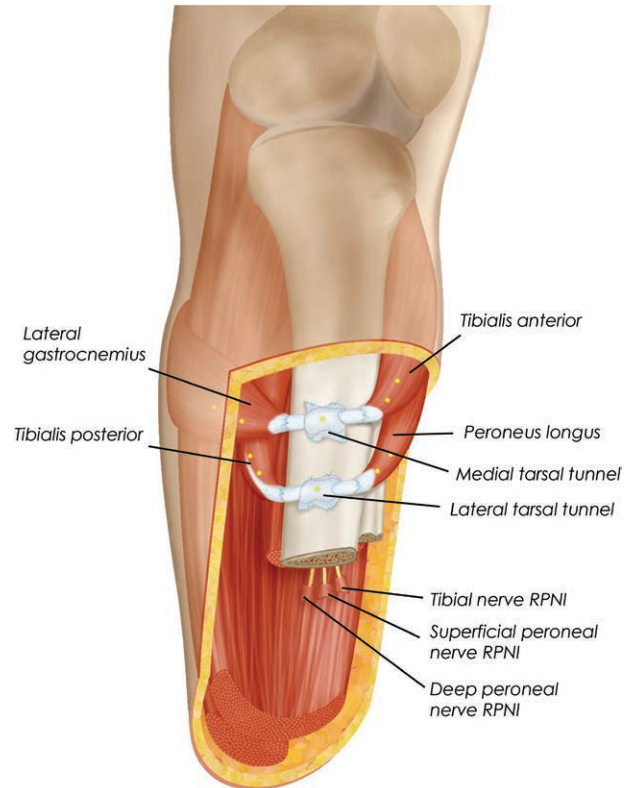


**Fig. 4.** Schematic illustration of the Ewing amputation. Two AMIs are constructed in the residuum at the time of primary transtibial amputation. Tarsal tunnels harvested from the amputated ankle joint are affixed to the medial flat of the tibia and serve as pulleys for the AMIs. When the patient is connected to a robotic prosthesis, the proximal and distal AMIs are myoelectrically linked to the prosthetic ankle and subtalar joints, respectively. In the diagram, suture points are denoted by blue crosses and tantalum beads are denoted by yellow circles. Positioning of these elements are representative, and not to scale.

dorsiflexion, peroneus longus activation minus tibialis posterior activation). Percent co-contraction was calculated as the proportion of antagonist muscle activation to agonist muscle activation, times 100%. For these experiments, performance of the AMI patient cohort was contextualized against a group of 3 persons with traditional transtibial amputations.

- **Ultrasound:** Although each subject cycled the phantom ankle joint, ultrasound was recorded on a portable high-definition scanner at 60 fps (LS128, Telemed) with the probe positioned adjacent to the proximal tarsal tunnel. EMG was simultaneously recorded from both the TA and the lateral gastrocnemius. Manual

tracking of the tantalum beads was used to generate a motion trajectory. All distance measurements were normalized to the length of each patient's medial tibial flat. These measurements were then cross-correlated with differential EMG amplitude (TA EMG minus lateral gastrocnemius EMG) to assess the relationship between muscle activation and tendon travel.

## RESULTS

The mean age of study participant was  $38 \pm 13$  years, with a mean body mass index of  $29.5 \pm 5.5$  kg/m<sup>2</sup>; complete patient demographics and operative metrics are shown in Table 1. Two subjects demonstrated transient residual limb cellulitis overlying the AMI constructs at 2 weeks postoperatively, requiring short course oral antibiotic therapy (Fig. 5A). One subject demonstrated delayed superficial wound healing at the surgical closure, requiring conservative topical wound care to achieve full healing by secondary intention. Two subjects developed nonpainful pseudobursae overlying their AMI constructs that did not require intervention (Fig. 5B). One subject required operative ablation of a tibial osteophyte unrelated to AMI construction approximately 1 year after the primary amputation.

All 3 patients tolerated physical therapy without issue and demonstrated full compliance for the duration of their therapy course. All were amenable to standard shrinker therapy and standard prosthesis fitting and demonstrated excellent independent ambulation following appropriate prosthesis training. Comparisons of preoperative and postoperative limb circumference measurements demonstrated mild hypertrophy at the level of the mid-tibia and osteotomy level (Table 1). Preservation of muscle bulk in the residual limb obviated the need for extended suspension systems in all subjects and required minor modifications to socket design to accommodate the modest mass effect of the AMI constructs in the anterior leg (Fig. 5C).

Radiologic imaging of each residual limb demonstrated stable construct positioning over time, as well as visible excursion of the AMI musculature as evidenced by fluoroscopy and high-resolution ultrasound [Fig. 6; see figure, Supplemental Digital Content 2, which displays fluoroscopy demonstrates motion of AMI constructs upon volitional activation by patient 1, as reflected by excursion of radiopaque tantalum beads, <http://links.lww.com/PRSGO/A912>; see figure, Supplemental Digital Content 3, which displays high resolution ultrasound demonstrates excursion of TA and lateral gastrocnemius AMI construct over anterior surface of tibia (T) in patient 1, <http://links.lww.com/PRSGO/A913>]. Functional testing demonstrated a high correlation between differential EMG amplitude and tendon travel ( $R = 0.94, 0.85, 0.95$  for patients 1–3, respectively;  $P < 0.0001$  for correlation) indicating coupled motion of the AMI constructs during volitional isolated movement of the phantom ankle joint (Fig. 7).

Simultaneous EMG recordings from the 4 AMI muscles during volitional motion in the 4 cardinal movement directions were repeatable across trials, and movement intent was clearly identifiable (Fig. 8A; see figure, Supplemental Digital Content 4, which displays surface EMG demonstrates independence of muscle activation during volitional motion of the phantom limb, <http://links.lww.com/PRSGO/A914>). For each motion, muscle activation from the AMI patients was more consistently isolated to the muscles associated with that motion than in the patients with traditional amputation, resulting in a significant reduction in antagonistic ( $P < 0.00001$ ,  $n = 60$  trials) and auxiliary ( $P < 0.0015$ ,  $n = 60$  trials) muscle activation (Fig. 8B). AMI patients demonstrated a significant reduction in unintended co-contraction (Fig. 8C) during plantar flexion ( $P < 0.02$ ,  $n = 60$  trials), dorsiflexion ( $P < 0.0005$ ,  $n = 60$  trials), and eversion ( $P < 0.0005$ ,  $n = 60$  trials) compared with the cohort of patients with

**Table 1. Study Subject Characteristics**

Measure	Patient 1	Patient 2	Patient 3	Mean	Standard Deviation
Age at surgery (y)	52.6	26.0	36.5	38	13
Sex	M	M	M	—	—
BMI (kg/m <sup>2</sup> )	25.9	35.9	26.8	29.5	5.5
Laterality	Left	Left	Left	—	—
Etiology	Fall	IED	Congenital	—	—
Prior operations	Multiple	Multiple	Multiple	—	—
Operative time (min)	269	440	330	346	87
Tourniquet time (min)	120	120	120	120	—
Fluids (cc)	1,000	2,700	1,100	1,600	954
EBL (cc)	150	300	150	200	87
UOP (cc)	240	500	800	513	280
LOS (d)	6	4	4	5	1
Drain removal (d)	17	14	20	17	3
Suture removal (d)	35	43	27	35	8
Prosthesis fitting (d)	35	43	27	35	8
Limb circumference measurements					
Preoperative MTC (cm)	32	38	30	33	33
Postoperative MTC (cm)	32	39.5	30.5	34	34
Preoperative DTC (cm)	28	37	32	32	32
Postoperative DTC (cm)	28	39.5	31	33	33
MTC relative difference (%)	100	104	102	102	102
DTC relative difference (%)	100	107	97	101	105

BMI, body mass index; DTC, distal tibial circumference; EBL, estimated blood loss; LOS, length of stay; MTC, mid-tibial circumference; UOP, urine output.



**Fig. 5.** Postoperative sequelae. A, Mild cellulitis was noted overlying the AMI constructs in 2 subjects 2 weeks after amputation; both resolved with oral antibiotic therapy. B, Development of a nonpainful pseudobursa overlying the AMI constructs was noted in 2 patients. C, Preservation of muscle bulk in the residual limb and slight prominence of AMI constructs required minor modifications in prosthesis socket design for all three study subjects.

traditional amputation. No significant difference was observed for inversion ( $P > 0.5$ ,  $n = 60$  trials); all patients from both groups anecdotally reported having difficulty isolating the inversion movement.

Subjective reporting by each subject revealed full sensation of joint movement across the ankle and subtalar joints. Perhaps the most compelling anecdotal evidence is that of patient 3, who, because of his congenital ankle defect, had never before experienced the full range of ankle and subtalar joint motion. Three months after his primary amputation surgery, this patient reported new percepts of

joint motion across the full range of his joint space. He described a feeling of “completeness” associated with this newfound perception of full joint mobility.

### DISCUSSION

This case study demonstrates the potential of the Ewing amputation to benefit persons with transtibial amputation, irrespective of their chosen prosthetic system. It is our hypothesis that each of these benefits can be attributed to the AMI’s unique preservation of dynamic agonist-antagonist muscle relationships.

Significant muscular atrophy was not observed within the residual limb of any of the AMI patients. One potential explanation for this outcome is that the lack of isometric



**Fig. 6.** Plain radiograph of residual limb. Radiopaque tantalum beads illustrate intact position of AMI constructs in the residuum, 6 weeks after the operative procedure.

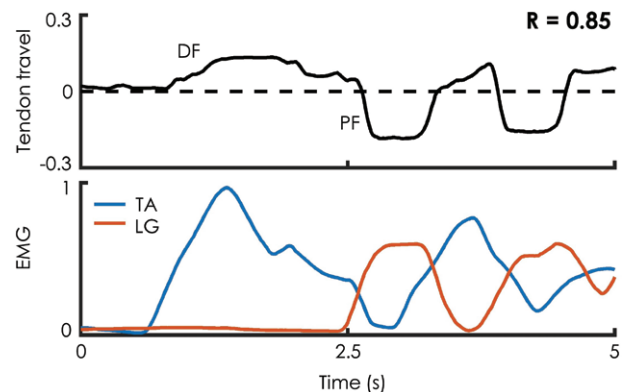


**Fig. 7.** Ultrasound evidence of dynamic AMI muscle relationships. Patients were asked to cyclically move the phantom ankle from approximately 80% dorsiflexion through approximately 80% plantar flexion, while ultrasound from the proximal tarsal tunnel and EMG from AMI muscles were simultaneously recorded. A representative sample is shown from patient 2. Tendon travel measurements are normalized to the length of the patient’s medial tibial flat. EMG values are normalized to the maximum EMG recorded from a given trial.

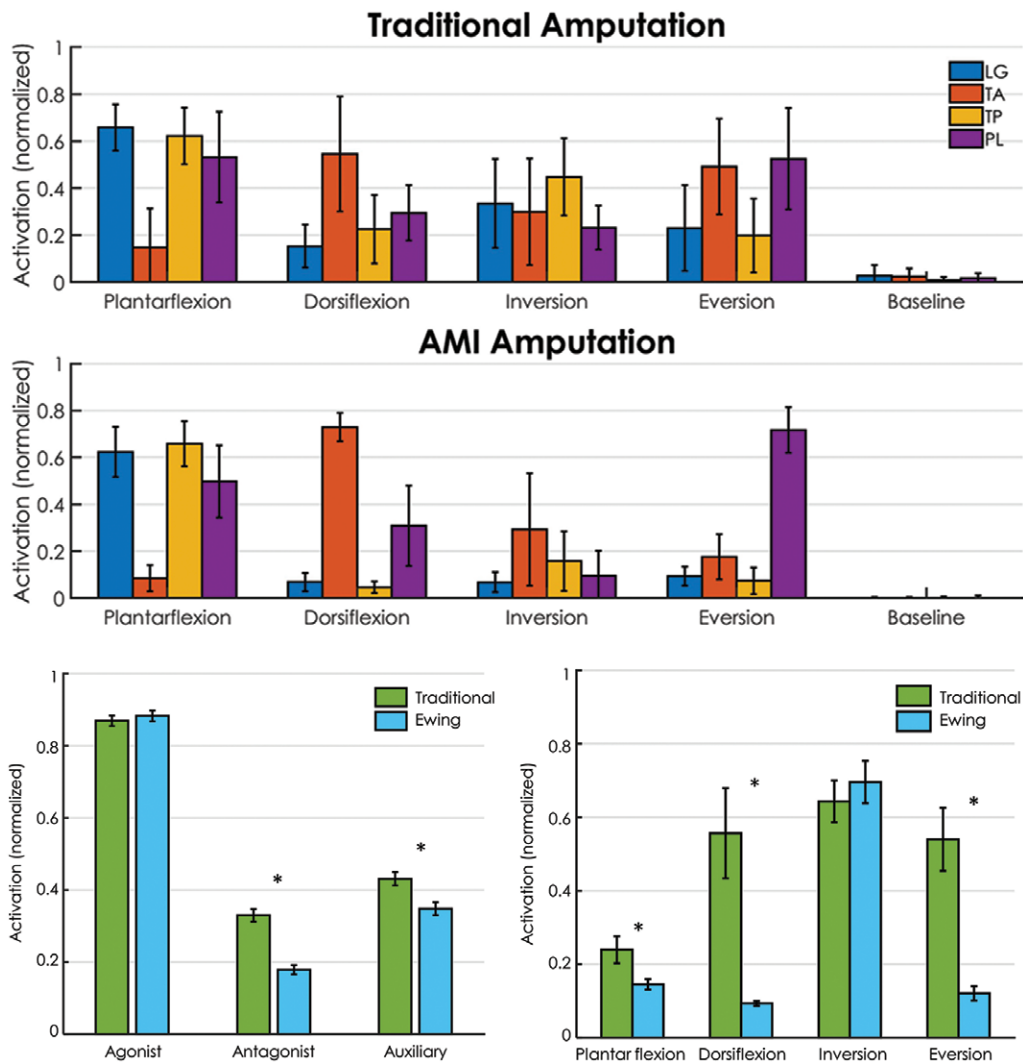


**Fig. 8.** EMG amplitude during volitional movement of the phantom limb. AMI patients showed a repeatable generation of activation in muscles typically associated with each desired movement (A), an improved ability to limit muscle activation in muscles not associated with the desired movement (B), and a decrease in unintended co-contraction (C). Error bars depict standard error. Asterisk indicates significant difference at  $\alpha = 0.02$ .

fixation of the muscles within each patient’s residuum enables concentric, eccentric, and isometric muscular contractions. Nonisometric muscle loading has been shown to play a key role in maintaining and increasing muscle mass.<sup>16</sup> Another potential explanation is that the repeatable proprioceptive affirmation of muscle activity that accompanies each volitional or reflexive contraction of an AMI muscle may preserve natural firing patterns during activities of daily living.

None of the 3 patients that received the Ewing amputation reported pathological neural symptomatology from their phantom ankle or subtalar joints. In a traditional amputation, the afferent mechanisms that mediate proprioceptive sensation are disrupted when the mechanical coupling between opposing muscles is severed. The AMI prevents the disruption of these mechanisms by preserving the natural relationships between muscle spindles and Golgi tendon organs in antagonistic muscle pairs. We hy-

pothesize that maintenance of these key muscle relationships is essential to avoiding aberrant phantom sensation and preventing the chronic neurological remapping that has been identified as a predominant cause of phantom pain.<sup>17–19</sup> Future studies with a larger patient cohort are planned to fully evaluate this hypothesis. Neither patient 2 nor 3 reported phantom sensation localized to distal cutaneous tissues; it is believed that the lack of cutaneous phantom symptomatology in these 2 patients may be a result of RPNI creation on all nerves transected during amputation.<sup>20</sup>

One of the primary benefits of the Ewing amputation lies in its potential to improve bi-directional neural control of advanced bionic limbs. It is in concert with a coherently and complementarily designed advanced prosthetic limb that the procedure reaches its fullest potential.<sup>14</sup> All 3 subjects demonstrated an ability to generate discrete neural commands associated with movement of their phan-

tom joints. A result of particular interest is the reduction in unintended co-contraction during volitional muscle activation. This is consistent with anecdotal reporting in a previous study<sup>14</sup> and demonstrates the potential of the AMI to restore the reciprocal inhibition reflexes that are essential to joint control.<sup>21–23</sup> Each patient also described persistent natural sensations of joint movement across the range of their phantom joint space associated with volitional activation of the AMI muscles.

The primary limitations of this work are those typical of a pilot study. Data are only presented from a small number of patients; therefore, no statistical claims can be made about the relative benefits of the Ewing amputation as compared with a traditional transtibial amputation. To address this limitation, a case-control, prospective clinical trial is currently underway.

The Ewing amputation is described as an elective procedure at the transtibial level; as such, AMI construction in the current implementation is dependent on availability of soft tissues distal to the amputation site. This feature of the surgical architecture limits accessibility of the Ewing amputation to persons in whom the requisite distal tissues are readily available. Modifications to this procedure would be necessary, for instance, in the case of residual limb repair following traumatic below knee amputation. In light of this limitation, we have demonstrated in other studies an approach by which AMIs can be constructed in revision procedures, or in primary amputation scenarios in which distal soft tissues have been significantly compromised, by leveraging the regenerative properties of nerves and muscles.<sup>12,15</sup> In addition, although the Ewing amputation is described only at the transtibial level, AMIs can be implemented at all levels and locations of amputation. Methodologies are being explored by which AMIs can be constructed at the time of primary transfemoral, transradial, and transhumeral amputations. These techniques have the potential to significantly expand applicability of the AMI.

## CONCLUSIONS

Traditional limb amputation surgery is technically simple and has historically been associated with limited functional outcomes, casting it as a therapy of last resort to be considered only when all other attempts at limb salvage have failed. The Ewing amputation is a first step toward redefining the notion of amputation from one of surgical failure to an alternative form of limb salvage.

**Matthew J. Carty, MD**

Division of Plastic Surgery  
Brigham and Women's Hospital  
75 Francis St  
Boston, MA 02115  
E-mail: mcarty@bwh.harvard.edu

## REFERENCES

- Herr H, Clites T, Srinivasan S, et al. Limb loss as salvage: reinventing amputation for the 21st Century. 2018.
- Souza JM, Cheesborough JE, Ko JH, et al. Targeted muscle reinnervation: a novel approach to postamputation neuroma pain. *Clin Orthop Relat Res*. 2014;472:2984–2990.
- Brown BJ, Iorio ML, Klement M, et al. Outcomes after 294 transtibial amputations with the posterior myocutaneous flap. *Int J Low Extrem Wounds*. 2014;13:33–40.
- Kuiken T, Li G, Lock B, et al. Targeted muscle reinnervation for real-time myoelectric control of multifunction artificial arms. *JAMA*. 2009;301:619–628.
- Hargrove LJ, Simon AM, Young AJ, et al. Robotic leg control with EMG decoding in an amputee with nerve transfers. *N Engl J Med*. 2013;369:1237–1242.
- Baldwin J, Moon J, Cederna P, et al. Early muscle revascularization and regeneration at the regenerative peripheral nerve interface. *Plast Reconstr Surg*. 2012;130:73.
- Urbanek M, Baghmanli Z, Wei B, et al. Long-term stability of regenerative peripheral nerve interfaces (RPNI). *Plast Reconstr Surg*. 2011;128(4S):88–89.
- Kung TA, Langhals NB, Martin DC, et al. Regenerative peripheral nerve interface viability and signal transduction with an implanted electrode. *Plast Reconstr Surg*. 2014;133:1380–1394.
- Herr HM, Riso RR, Song KW, et al. Peripheral neural interface via nerve regeneration to distal tissues. US20160346099. 2016.
- Herr HM, Clites TR, Maimon B, et al. Method and system for providing proprioceptive feedback and functionality mitigating limb pathology. 2016;62.
- Clites TR, Carty MJ, Srinivasan S, et al. A murine model of a novel surgical architecture for proprioceptive muscle feedback and its potential application to control of advanced limb prostheses. *J Neural Eng*. 2017;14:036002.
- Srinivasan SS, Carty MJ, Calvaresi PW, et al. On prosthetic control: a regenerative agonist-antagonist myoneural interface. 2017;2:eaan2971.
- Clites TR, Carty MJ, Herr HM. A caprine model of a novel amputation paradigm for bi-directional neural control of a bionic limb. *Plast Reconstr Surg Glob Open* 2017;5(4S):119.
- Clites TR, Carty MJ, Ullauri JB, et al. Proprioception from a neurally controlled lower-extremity prosthesis. *Sci Transl Med*. 2018;10:eaap8373.
- Srinivasan S, Diaz M, Carty M, et al. Towards functional restoration for persons with limb amputation: a dual-stage implementation of regenerative agonist-antagonist myoneural interfaces. 2018.
- Higbie EJ, Cureton KJ, Warren GL 3rd, et al. Effects of concentric and eccentric training on muscle strength, cross-sectional area, and neural activation. *J Appl Physiol (1985)*. 1996;81:2173–2181.
- Flor H, Elbert T, Knecht S, et al. Phantom-limb pain as a perceptual correlate of cortical reorganization following arm amputation. *Nature*. 1995;375:482–484.
- Flor H, Nikolajsen L, Staehelin Jensen T. Phantom limb pain: a case of maladaptive CNS plasticity? *Nat Rev Neurosci*. 2006;7:873–881.
- MacIver K, Lloyd DM, Kelly S, et al. Phantom limb pain, cortical reorganization and the therapeutic effect of mental imagery. *Brain*. 2008;131:2181–2191.
- Woo SL, Kung TA, Brown DL, et al. Regenerative peripheral nerve interfaces for the treatment of postamputation neuroma pain: a pilot study. *Plast Reconstr Surg Glob Open*. 2016;4:e1038.
- Smith AM. The coactivation of antagonist muscles. *Can J Physiol Pharmacol*. 1981;59:733–747.
- De Luca CJ, Mambrito B. Voluntary control of motor units in human antagonist muscles: coactivation and reciprocal activation. *J Neurophysiol*. 1987;58:525–542.
- Dimitriou M. Human muscle spindle sensitivity reflects the balance of activity between antagonistic muscles. *J Neurosci*. 2014;34:13644–13655.